

## PATCH LOADING IN SLENDER AND HIGH DEPTH STEEL PANELS: FEM - DOE ANALYSES AND BRIDGE LAUNCHING APPLICATION

**Antonio Navarro-Manso<sup>1</sup> Juan José del Coz Díaz<sup>2\*</sup>, Mar Alonso-Martínez<sup>2</sup>, Daniel Castro-Fresno<sup>3</sup> and Felipe Pedro Alvarez Rabanal<sup>2</sup>**

<sup>1</sup> *Department of Energy, University of Oviedo, 33204 Gijón (Spain)*

<sup>2</sup> *Department of Construction, EPSIII, University of Oviedo, 33204 Gijón (Spain)*

<sup>3</sup> *GITECO Research Group, ETSICCP, University of Cantabria, 39005 Santander (Spain)*

### 1. Introduction

The bridge launching construction system assembles the deck of the bridge in a location or position different than the definitive one; by means of adding successive segments, the deck is launched forward on the piers and other supplementary supports. Many auxiliary systems are usually used with the aim of resisting the huge forces in the cantilever section (bending and torsional -if any- forces and point loads); as well as pushing systems to propel the deck forward (see Fig. 1).

This method allows the construction of the bridge to be highly independent of the ground conditions. The launching method (today Incremental Launching Method, ILM) was developed in Europe in the Nineteenth Century, as it was exposed in some research works and Thesis [1]. This erection method was applied mostly to steel bridges (e.g. Neuvial Viaduct, by G. Eiffel, 1869, France). Nevertheless it was not until the mid-Twentieth Century that the best examples were constructed. The Caroni Bridge, over the Caroni River in Venezuela built in 1961, by Leonhardt and Baur, is considered to be the first modern application of this method, launching in this case a concrete bridge. The patent of this method is dated to 1967 [2].

---

\* Corresponding Author: Prof. Juan José del Coz Díaz  
Email: [Juanjo@constru.uniovi.es](mailto:Juanjo@constru.uniovi.es)

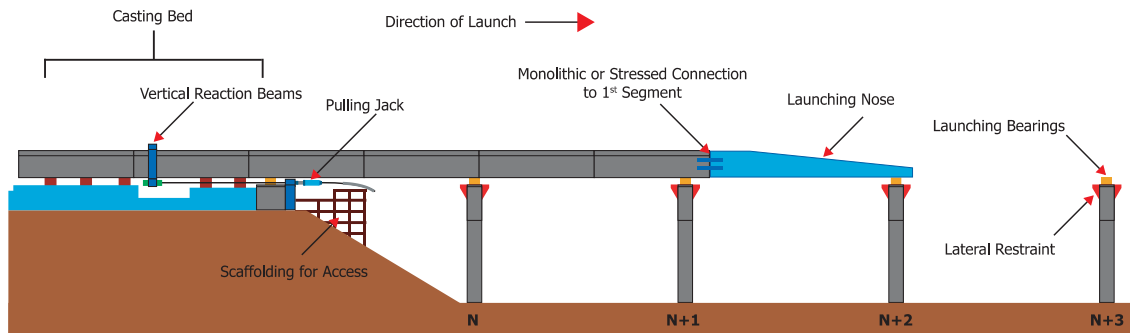


**Fig.1.** Launching conventional method scheme with nose and cable pulling system (courtesy of VSL Ltd.).

### 1.1 Bridge launching present disadvantages

Despite this method's multiple advantages, which have led this system to become widespread all over the world in the past three decades, the method presents some problems that may make it less competitive compared to other construction systems, depending on the bridge and site characteristics.

State of the Art methods [3,4] have presented a wide range of alternatives for launching bridges. The limitations of those techniques are described below:

- The structure is subjected to two very different resistance schemes: the cantilever beam during the construction stages and the continuous beam during the service life. Usually Serviceability Limit States (SLS) during construction are more restrictive than the final conditions [5].
- Every section must resist alternate sign bending forces and patch loading, even the sections that have not been designed to do so when the construction is completed. This is a critical factor in designing the first two spans of the bridge [6].
- There is some preparation time because of the need to set up the auxiliary and pushing systems, and the launching speed is not fast [7].
- It is difficult to have a good safety system in order to control or monitor reactions on every support during the launching, and to achieve the compensation of the load is not currently available [8].
- This construction method is not very sustainable because it uses a lot of non-reusable materials [9].
- Finally, safety is sometimes compromised because the current pushing system is not reversible and does not allow the deck to retract fast and easily [10].

## 2. The new launching method

The new method for bridge launching is patent-protected [11,12] and allows the use of longer spans, which are easier and cheaper than the ones used nowadays. The main issue

in such structures is related to the patch loading phenomenon that may produce the instability of slender steel webs.

## 2.1 Patch loading solutions in conventional ILM

The 150 m long cantilever presented in this paper implies a huge point load directly on the supports of the first pier. This action is named patch loading in the specialized literature and it is one of most important design problems when regarding slender steel plates, because the yield resistance of the steel cannot be fully taken into account and instability phenomena, like buckling, drastically decrease the ultimate load that panels can resist.

The most important factor that contributes to resist point loads is the thickness of the web. Other parameters that have an influence on the patch loading phenomenon are the position of the support with respect to the web axis, the stiffeners located all along the deck, the disposition of transversal frames and the steel strength.

The benefits of designing longitudinal and vertical stiffeners are well known, thus the steel plate is divided into sub-panels that can reduce the transversal displacement. Almost all the international codes and rules need to adopt simplifications in order to attain an expression that could be useful. This is one of the reasons why these expressions must be checked through experimental data, testing different boundary conditions of the steel plate, several ways to apply the load, etc.

One of the most common theoretical works is the Lagerqvist model, generally considered as the basis of the technical rules used for designing steel bridges [13,14]. Other authors [15, 16] has been studied different typologies for longitudinal stiffeners and the failure mechanism under patch loading (see Fig. 2).

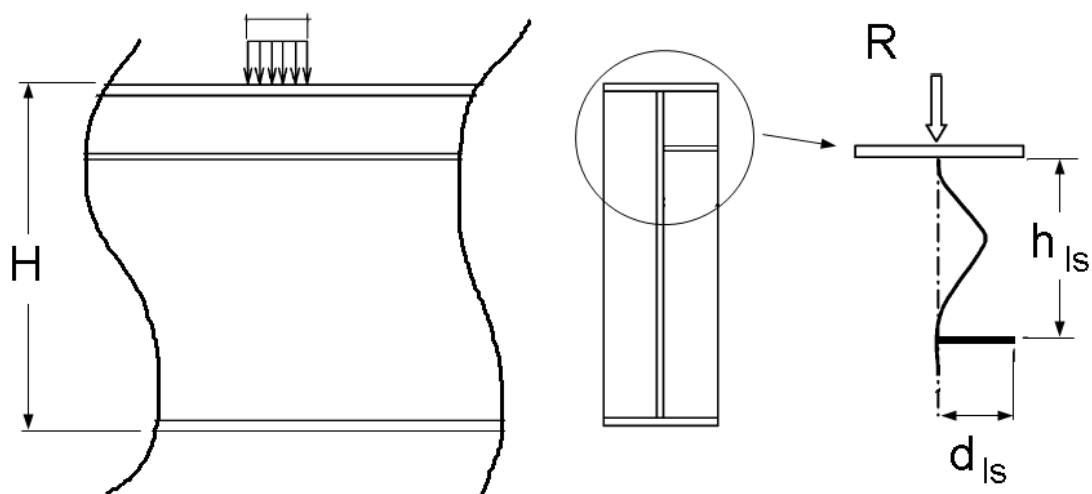


**Fig. 2.** Typical failure mechanism of longitudinally stiffened slender girder under patch loading.

However these methods and experimental data cannot accurately solve special configurations, like the configuration hereby described containing the triangular cell neither the actual boundary conditions nor the influence of longitudinal and transversal stiffeners in a high depth steel plate under the huge patch loading and bending moment actions; nor the interaction of all the phenomena involved [17,18].

## 2.2 Description of the proposal

The new patented launching method (see Fig. 3) allows launching steel bridges up to a span length of 150 m. No auxiliary means are needed because the main structure of the deck itself is used as reinforcement of the weakest sections during the construction stage. This method is called New Bridge Launching Method (NBLM) [19].

The first two spans of the deck have a special configuration that consists of the positioning of the last span of the bridge directly on top of the deck launched. These pieces must be joined (for instance by High Strength Friction Grip bolts, HSFG) to ensure they are working together and so bending moments, shear forces and patch loading phenomenon can be safely resisted. No section is oversized and important savings (in terms of cost and time) may be achieved. Specific longitudinal and transversal stiffeners are designed because they play a decisive role in the behaviour of the deck during both construction and service stages. During the final construction phase the double deck is removed and installed in its definitive location, the last span of the bridge.

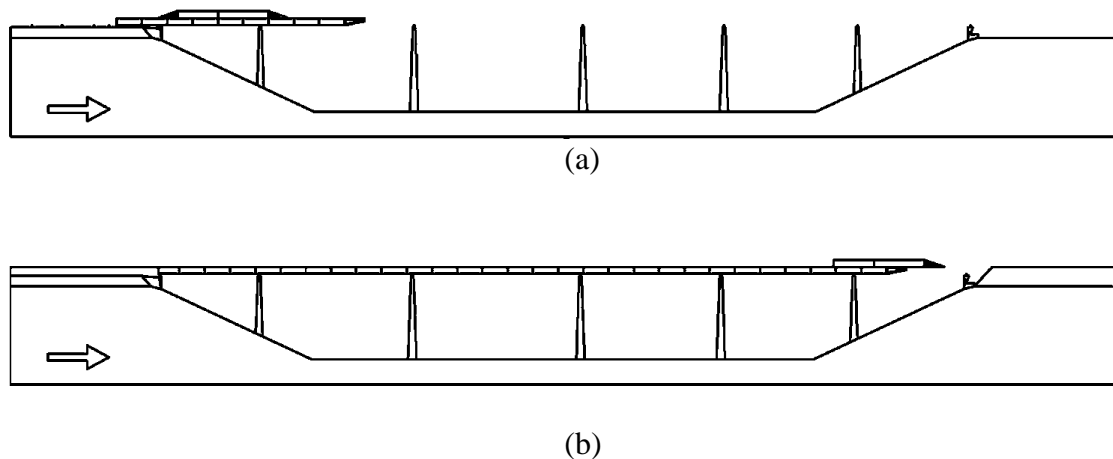


**Fig. 3.** New launching method: (a) launching phase overview; and (b) assembly of the double-deck over the last span.

The system described and shown above is completed with other mechanisms, such as the small nose to reduce and regain the deflection during the largest launching phase, disconnection system of the double-deck and the new device for continuous bridge launching [20].

### 2.3 Advantages

The main advantages of the new method are the following [19,21]:

- Critical sections, mostly those belonging to the first span during the launching, do not have to be oversized with respect to requirements of the serviceability limit state.
- Launched span is increased and no auxiliary means are needed.
- Material is more efficiently and sustainably used, only when it is needed.
- Torsional behavior of the deck, and the general structural behavior, during the launching are improved; even when curved geometries are assembled.
- The construction process involves simple and repetitive operations that can be monitored. The increasing of the span allows the protection of the environmental surroundings of the location. All of this leads to a lower execution time and costs, as well as to a better quality of work.

## 3. Numerical models

The numerical simulation was carried out using a nonlinear finite element model (FEM). The structural response of the basic parts making up the bridge is understood in great detail thanks to this simulation technique, saving costs and time in relation to tests [22].

Only the first two spans of the bridge are modeled since the behavior of the whole deck can be simulated accurately by adding the corresponding boundary conditions. The FEM model used includes the main cantilever span of 150 m and the adjacent span from pier nº 1 to the abutment. So this model corresponds to the critical phase launching and is 280 m long.

### 3.1 Finite element model

The FE model in this work has been based on the ANSYS software [22], using the following element types and contacts (see Fig. 4):

- SHELL 181 is a kind of element used to model thin walled structures, like steel plates (including webs, flanges and stiffeners). It is well suited for linear, large rotation, and/or large deflection nonlinear applications and is a three-dimensional four node finite element having six degrees of freedom per node: translations and rotations in the nodal X, Y, and Z directions.
- The finite element SOLID186, used to model the plates of the bearings, is a higher order 3D 20-node solid that exhibits quadratic displacement performance having three degrees of freedom per node: translations in the nodal X, Y, and Z directions.

- Contact model: in order to reproduce the relationship that exists between all the bodies, we have considered a bonded contact type through the "Pure Penalty" algorithm [22]. Thus the real behavior of the welded joints is correctly simulated.

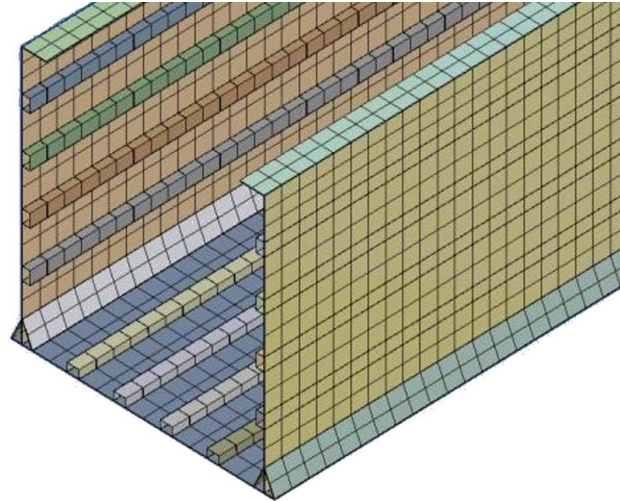


**Fig. 4.** Typical mesh of shell elements in the box girder.

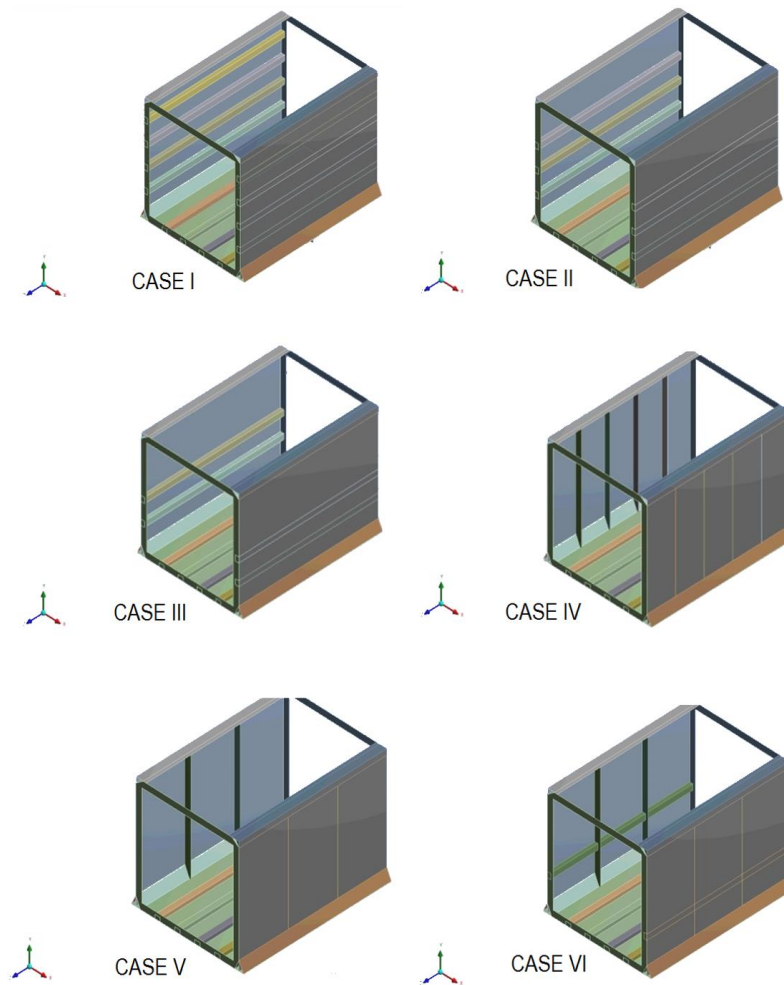
#### 3.1.1 Box girder, longitudinal stiffeners, transversal frames and triangular cell

The main box girder and the double-deck is composed of two 7 m high plates and the bottom plate that is 7 m wide (Fig. 5). A triangular cell of 0.5 m to 0.6 m high runs along the whole structure, just below each web. This makes a strong longitudinal stiffener at the loaded head of the vertical plates and its optimum position is about 10% of total depth (Figs. 5b and 5c) [23].

General transversal stiffness is achieved by means of frames  $20 \cdot 10^{-3}$  m thick separated 10 m along the longitudinal axis. Six different FEM models were analysed, all of them containing the triangular cell along the lower flange. Variations in the distribution of the stiffeners (maintaining constant the configuration of the bottom plate) are described below (see Fig. 5a):

- CASE I: 4 longitudinal stiffeners  $8 \cdot 10^{-3}$  m thick along the webs. Cross section is closed and dimensions are 0.350 x 0.230 m. Thus the stiffeners are separated by about 1 m.
- CASE II: 3 longitudinal stiffeners along the webs, with the same geometric characteristics and located in the lower half of the girder depth, thus separation between stiffeners is 1 m again.
- CASE III: 2 longitudinal stiffeners along the webs, located at 1.7 m and 1 m above the bottom plate.
- CASE IV: 4 vertical stiffeners  $10 \cdot 10^{-3}$  m thick between two consecutive transversal frames. The cross section is open with a width of 0.4 m and they are located each 2 m in the longitudinal direction.

- CASE V: 2 vertical stiffeners between two consecutive transversal frames, with the same settings, separated by 3.33 m
- CASE VI: 1 longitudinal stiffener along the webs and 2 vertical stiffeners between two consecutive transversal frames. The characteristics of each stiffener have already been described and the longitudinal stiffener is 2 m above the bottom plate.



(a)

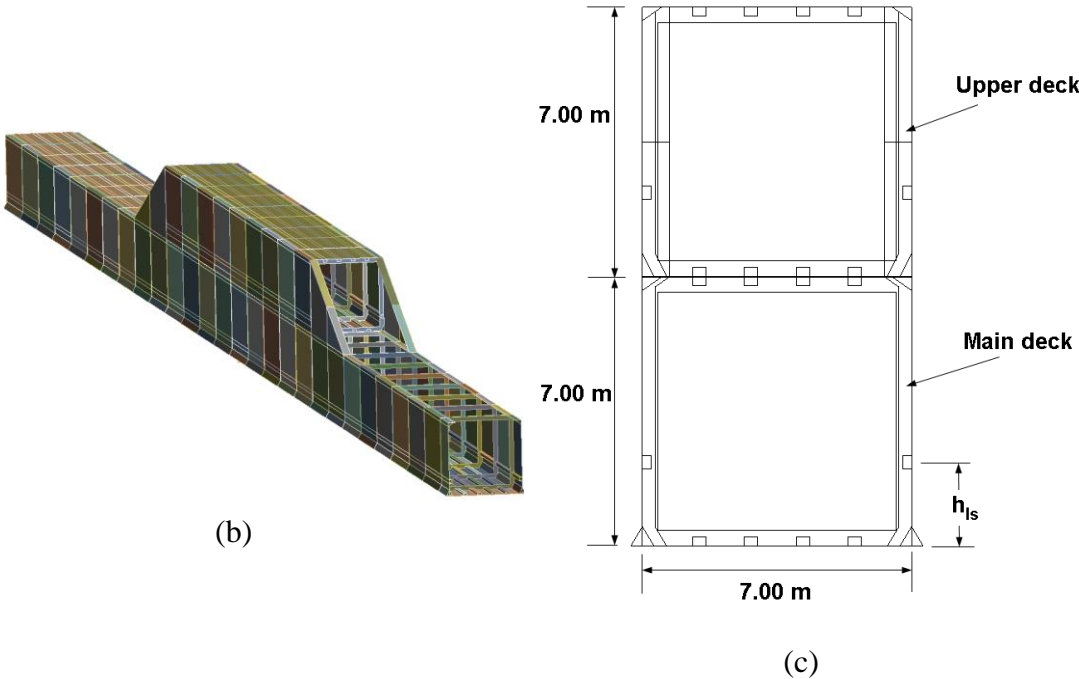


**Fig. 5.** Geometrical models: (a) CASE-I to CASE-VI stiffeners distribution, (b) FE model overview and (c) cross section of the middle part of the box girder for CASE VI.

*3.1.2 Launching bearings*

The supports are two rectangular (1.0 x 0.6 m) plates, simulating the behaviour of a real launching bearing. The geometrical model is meshed by a hex dominant method with a meshing parameter is 0.03 m. This method uses advanced meshing algorithms to allow the most appropriate cell type to be used to generate body-fitted meshes for the most general CAD geometries such as the bridge bearings in our case.

The plate stiffness composing the supports has been calculated with the objective of accurately reproducing the behaviour of a real launching support [24].

*3.1.3 Material properties, loads and boundary conditions*

- Material properties: the steel material model is defined as a bilinear plasticity model, with isotropic hardening. The corresponding elastic properties are summarized in Table 1 taking from ASME BPV Standard Rule, Section 8, Div. 2 [25].

**Table 1:** Material Properties of S-275 steel grade [25]

item	value	unit
Poisson’s ratio	0.3	



Elastic modulus	$2 \cdot 10^{11}$	Pa
Elastic yield strength	250	MPa
Tensile ultimate strength	460	MPa
Tangent modulus	10,000	MPa

---

- Loads and boundary conditions: in order to reproduce the structural behavior of the bridge during the critical launching phase, i.e. when the nose launching is arriving at the top of pier nº 2, we have considered the following (see Fig. 6):
  - A value of gravitational acceleration of  $9.81 \frac{m}{s^2}$  value
  - Bending moment at the rear of the deck of  $10^7$  N·m, based on a previous two-dimensional [11,19] analysis in which every force reaction on each pier was obtained. Shear force at the rear of the deck is directly absorbed by the supports.
  - The two launching bearings described in section 3.1.2, at pier nº 1, in which the rotational angle has been controlled by means of the stiffness of the vertical plate and also compared with previous 2D analysis. Vertical displacements are not allowed and horizontal movement is avoided in one of the bearings.
  - Simple support at the rear of the deck, 130 m long for pier nº1, precisely on the abutment and near the pushing system location, in which displacements are not allowed.

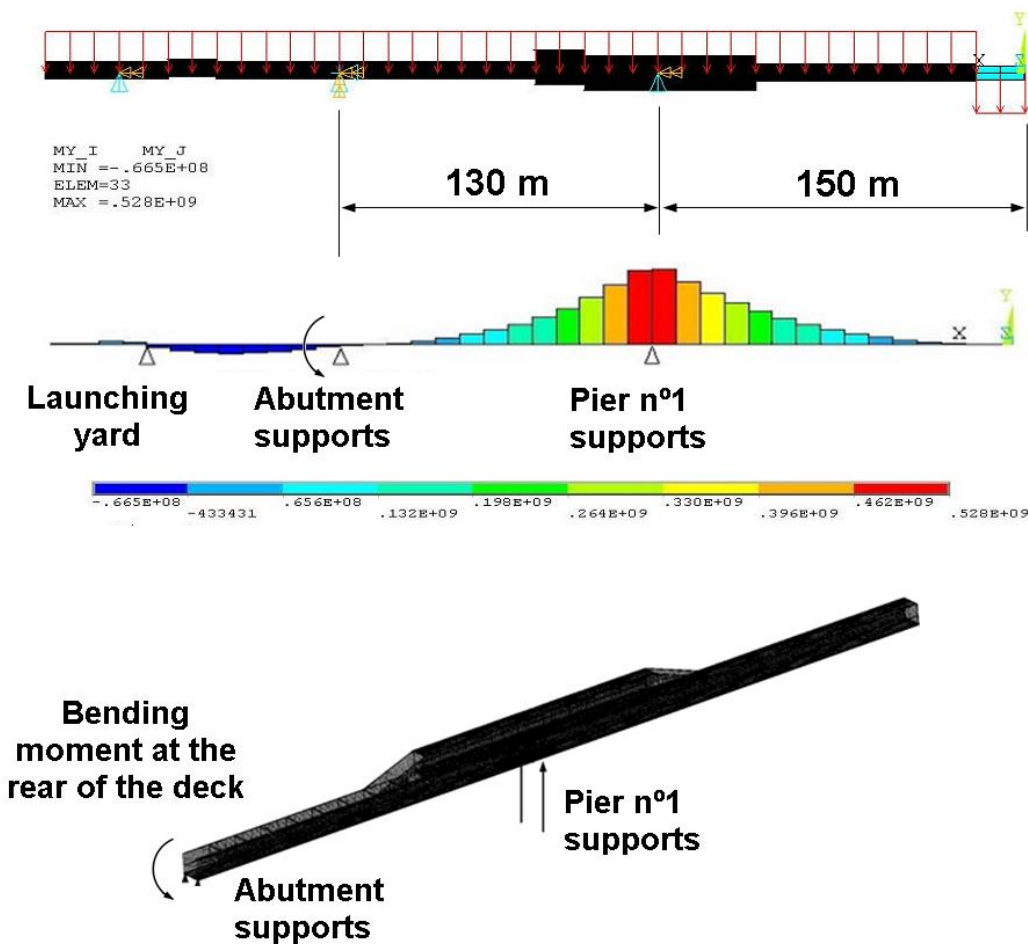


**Fig. 6.** Boundary conditions applied to the model.

### 3.2 Numerical analysis of the structural system

The present nonlinear static structural problem was solved by using the full Newton-Raphson option for all degrees of freedom with a non-symmetric solver including the adaptive descent option. With the aim of achieving an initial solution for the lineal buckling analysis it was necessary to perform a linear static structural analysis. Then a linear buckling analysis was undertaken and the normalized values of the initial defect of each mode were calculated. Finally, the plasticity of the material and actualization of the geometry in every step load was taken into account to obtain the failure load. To ensure the convergence of the results, the Newton-Raphson analysis options for a time step of 1 second, neglecting the inertial effects, are summarized in Table 2:

**Table 2:** Newton-Raphson analysis setting options for a time step of 1 second.

Item	value
------	-------

Initial Time Step [s]	0.1
Min Time Step [s]	0.001
Max Time Step [s]	0.1

A force tolerance value of 0.5% was considered with a minimum value of 0.01 N for stabilising the solution. The problem was solved on an INTEL Core i-7 64 bits processor, with 12 GB of RAM and 4 TB of hard drive. The CPU total time in each load case varied from 2.000 to 8.000 seconds for the full simulation of every case.

### 3.2.1 Linear Buckling Analysis

In this section the six cases with different stiffener distributions are calculated, in order to complete the design of the deck that is going to be launched. The numerical model used to calculate the deck stiffness and to considerer the non-linear effects includes the optimum triangular cell and the double deck system, both were mentioned above.

The model used for the analysis is supported by means of two provisional launching bearings described previously and they are located on pier nº1 at 145 m from the nose. This is the most critical launching phase in which the nose gets closer to pier nº 2 and the support bearings are located directly in the middle of two transversal frames. This condition will be investigated in the final design in order to assess the most critical location of the supports.

The linear buckling problem is solved by Equation (1), and the eigenvalues are obtained:

$$([K] + \lambda_i \cdot [S]) \cdot \{\Psi_i\} = 0 \quad (1)$$

where  $\lambda_i$  are the load factors of each buckling mode,  $[K]$  and  $[S]$  are stiffness and stress sate matrices, respectively, and  $\{\Psi_i\}$  is the matrix displacement of the structure.

The critical load  $P_{i_{cri}}$  of each buckling mode is obtained the following expression (2), where load factor increases with the maximum load  $P_i$ :

$$P_i \times /_i = P_{i_{cri}} \quad (2)$$

The first buckling modes affecting the web and their corresponding load factors are represented in the Fig. 7, for each case previously defined. In each case, fourty buckling modes were calculated using the Lanczos algorithm, in order to achieve enough precision during the non-linear analysis.

**Author's post-print:** Antonio Navarro-Manso, Juan José del Coz Díaz, Mar Alonso-Martínez, Daniel Castro-Fresno and Felipe Pedro Alvarez Rabanal. "Patch loading in slender and high depth steel panels: fem - doe analyses and bridge launching application" *Engineering Structures* 83 (2015) 74–85.  
<http://dx.doi.org/10.1016/j.engstruct.2014.10.051>

314

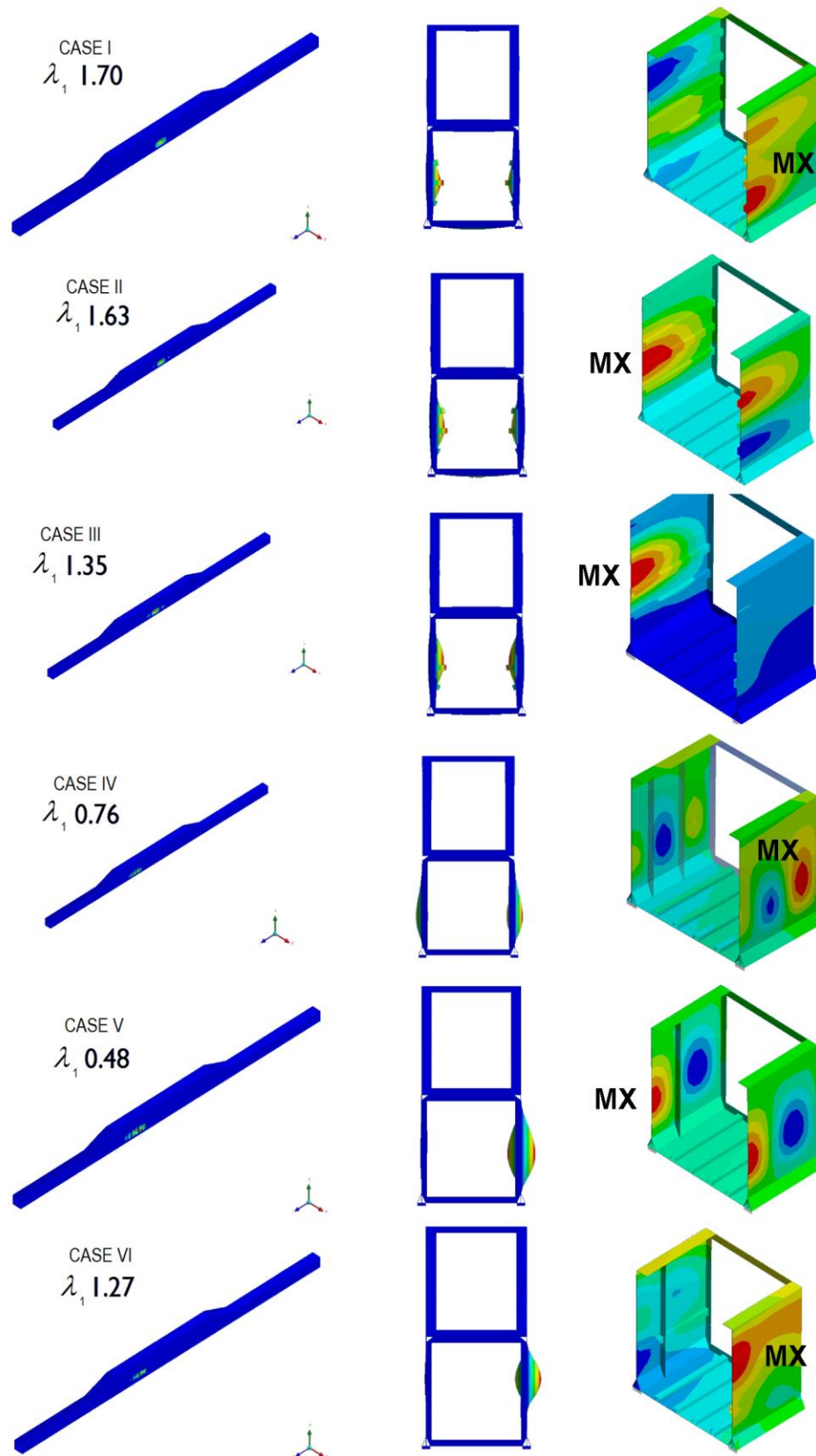


**Fig. 7.** From left to right, load multiplier, first mode and transversal displacements obtained for every stiffeners combination, CASE-I to CASE-VI (MX= maximum value).

The stability criterion used limits both the deflection of the web and the stress on every plate. The SLS must be accomplished and any plastic deflection is not allowed for the steel grade S-275 during the launching process. The condition for admissible transversal deflections, based on the usual deflection limit of simply supported beams under bending, is shown in Equation (3):

$$f_w = \frac{H}{300} = \frac{7}{300} = 0.023[m] \quad (3)$$

The results of the studied models are shown in the Table 3, numerical data is related to web plates.

**Table 3:** Results of stiffener design cases: I-III longitudinal, IV-V transversal and VI combined.

	I	II	III	IV	V	VI
Max. Deflection $f_w$ [m]	0.005	0.014	0.024	0.019	0.034	0.004
Max. Stress $\sigma$ [Pa]	$2.41 \cdot 10^8$	$2.43 \cdot 10^8$	$2.40 \cdot 10^8$	$2.41 \cdot 10^8$	$2.36 \cdot 10^8$	$2.32 \cdot 10^8$
1 <sup>st</sup> Load Multiplier $\lambda_1$	1.70	1.63	1.35	0.77	0.48	1.27
Failure	yield	yield	strain	yield	strain	ok
Critical element	web	web	web	web	cell	web

The most important observation from table 3 is that the stiffener distribution called CASE-VI, combining longitudinal and transversal stiffeners, and the triangular cell along the lower flange, is the best solution in bridges of long span (from the point of view of their construction system, i.e. launching), because the maximum deflection and von Mises stress are the least and the buckling load multiplier is greater than one. Also this stiffener distribution is appropriate in case of height decks larger than 4 m [10]. Besides maximum deflection occurs in the opposite panel with respect to the point load.

The next Section will explain the optimization of the whole system, including nonlinear effects.

### 3.2.2 Nonlinear analysis

The effective contribution of the general stiffening to the patch loading resistance is allowed in the codes used nowadays, but they only present a few cases and only take into

account the buckling of the directly loaded panel. In consequence the practical solution may be rather conservative or not correctly understood. So the non-linear analysis described in this paper can solve the buckling problem of the real case, accurately obtaining the collapsing load [25,26].

Once the linear buckling analysis has been carried out, the Case VI is selected to be solved under non-linear conditions. Eighteen linear buckling modes were combined by means of the Newton-Raphson algorithm. Fig. 8 shows the final von Mises stress of this case.

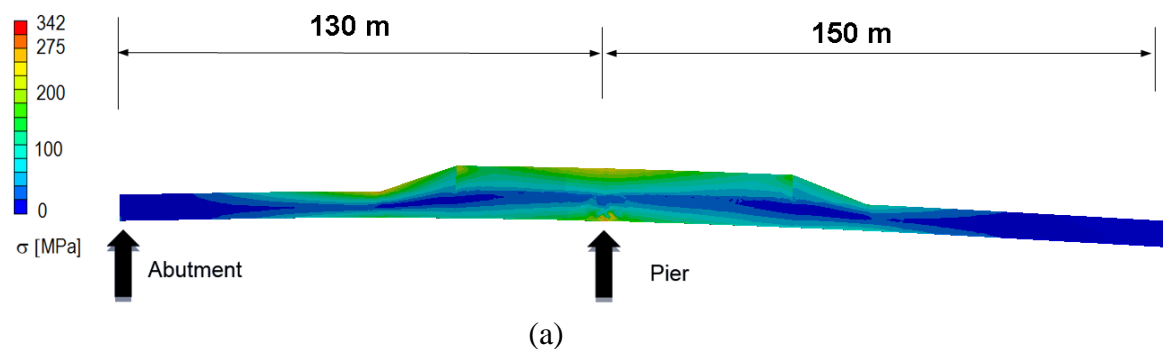
The FE code used does not include a specific module for this purpose, so an APDL code was written to solve the non-linear problem, taking into account the following [27-29]:

- Geometrical non-linearity: Eighteen linear buckling modes are combined.
- Material non-linearity: a bi-linear and isotropic model of plasticity with linear hardening.
- Large deflection: the model takes into account in each iteration the deflection of the structural element and the displacement of the load.

Thus, the initial imperfection (or tolerance of fabrication) that initiates the non-linear calculation is  $\frac{L}{500}$ ; this value is non-dimensionalized dividing it by the maximum displacement of each mode and multiplying by the percentage of the contribution of each local mode in the final deformation (see Equation (4)). This contribution has been distributed in a uniform way between those buckling modes that affect the deformation of the web.

$$w_i = \frac{\frac{l_i}{500}}{\max(f_{wi})} \cdot 1 \quad (4)$$

where  $i$  ranges from 1 to 18 - the local buckling modes which are considered -,  $l_i$  is the buckling length for each mode and  $\max(f_{wi})$  is the maximum deflection of each mode.



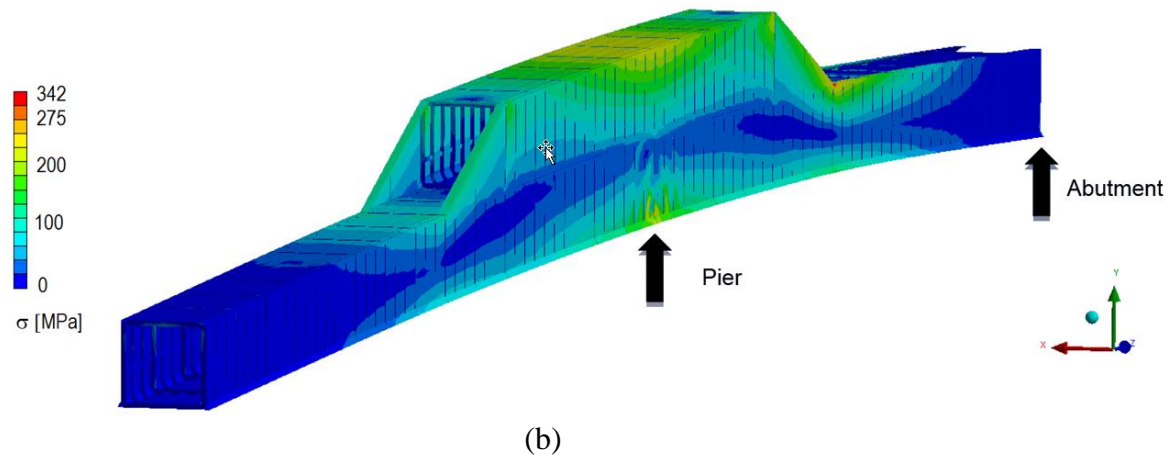


**Fig. 8.** von Mises stress result of the non-linear problem, 150 m long span, CASE-VI:  
(a) Longitudinal view. (b) Isometric view.

Once the general design has been carried out, the typology, the dimensions and the optimum position of the longitudinal stiffeners of the deck will be studied. The maximum von Mises stress result in webs is about  $2 \cdot 10^8$  Pa, lower than the steel yield strength limit. The patch loading phenomenon is controlled by the triangular cell and the general longitudinal stiffeners, bearing in mind the thickness of the web and cell plates. The model used allows the consideration of the interaction between patch loading and bending moment phenomena.

### 3.2.3 Optimization based on DOE analysis

Previously some different stiffener combinations have been analysed. The most efficient option, both technically and economically, is to place two vertical stiffeners and one longitudinal stiffener above the triangular cell. Thus, the instability of the web panel is highly controlled, the bearing load is well distributed and the von Mises stresses are lower than the yield stress of steel.

However, the simultaneous action of all the elements described nor there interaction have been taken into account yet. This final analysis shows how the new stiffening procedure works and the optimization of the most important parameters, such as the depth and the position of the stiffeners, are carried out. In order to verify the best triangular cell and stiffener combination the design of experiments (DOE) methodology has been used in this research work [30].

Firstly, the central composite design (CCD) was selected for the optimization of the parameters in the DOE methodology procedure [31,32]. Taking into account that the different variables are usually expressed in different units and have different ranges of variation, the importance of their effects on the structural behaviour can only be compared if they are coded.



Secondly, the DOE technique is an optimization approach permitting to determine the input combination of factors that maximize or minimize a given objective function [31]. Based on DOE and response surface method (RSM) the second order polynomial regression models can be developed to predict the performance of the structural system. Such numerical models are also known as response surface models (RS-models). During response surface modelling the input variables  $x_1, x_2, \dots, x_n$  must be scaled to coded levels. In coded scale the factors vary from  $(-1)$  that corresponds to minimum level up to  $(+1)$  that suit to maximum level. The second-order models given by RSM are often used to determine the critical points (maximum, minimum, or saddle) and can be written in a general form as [32]:

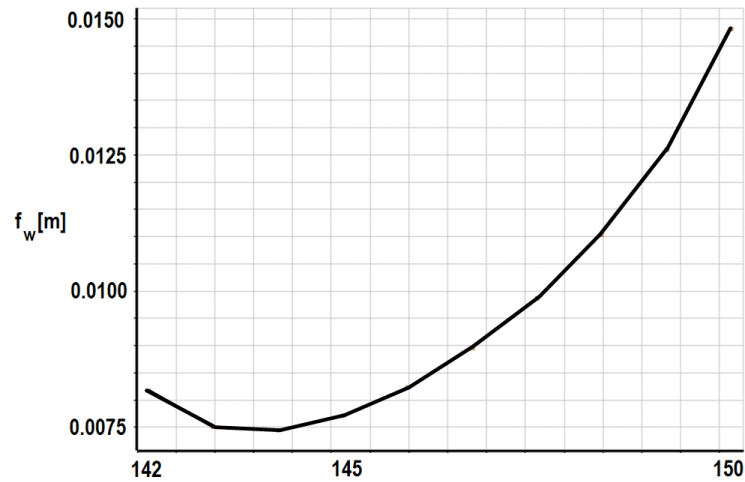
$$\hat{Y} = \beta_0 + \sum_{i=1}^n \beta_i x_i + \sum_{i=1}^n \beta_{ii} x_i^2 + \sum_{i < j}^n \beta_{ij} x_i x_j \quad (5)$$

where  $\hat{Y}$  denotes the predicted response,  $x_i$  refers to the coded levels of the input variables,  $\beta_0, \beta_i, \beta_{ii}, \beta_{ij}$  are the regression coefficients (offset term, main, quadratic and interaction effects) and  $n$  is the total number of input variables. To determine the regression coefficients of the Equation (5), the ordinary least squares (OLS) method is used.

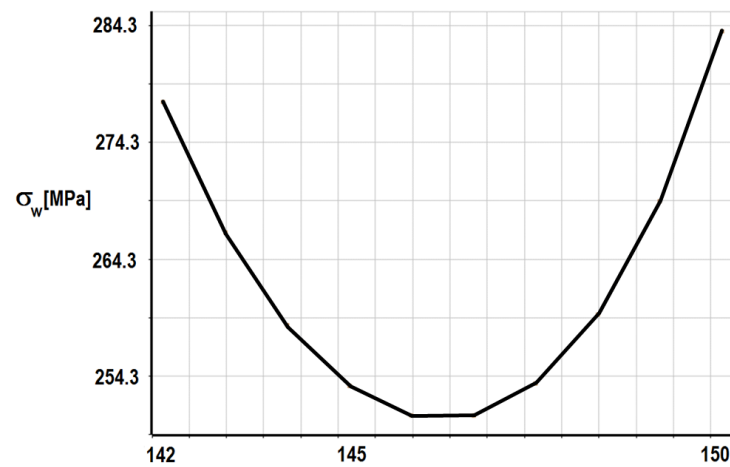
### 3.2.3.1 Critical position of the point load

When the bridge is arriving at the forward pier, the maximum cantilever is from 140 m to 150 m. This is the distance that one segment (10 m long) has to travel over the bearings from one transversal frame to the next. In order to study the patch loading phenomena, a step by step calculation has been carried out and the most problematic position of the bearings has been determined, taking into account the maximum load and the location of the bearings with regards to the transversal frames.

Besides the stress in the transversal frame and the vertical stiffeners themselves, the most important output parameter is the transversal deformation in the web; hence the stress in the transversal frame is always lower than the yield stress. The maximum deflection is reached when the total cantilever span is 150 m and the bearings are directly below the second transversal frame, as can be seen in Fig.9 (a).



(a)



(b)

**Fig. 9.** (a) Maximum displacement  $f_w$  in the web and (b) Maximum stress  $\sigma_w$  in the web vs total cantilever span length.

The next parameter affected by the bearing position is the maximum von Mises stress, taking into account the thickness of every plate before final optimization. Again the stress is critical when the cantilever span is 150 m. (See Fig. 9 (b)).

### 3.2.3.2 Triangular cell and web thickness optimization

The size and the thickness of this element, taking into account the whole model and the interaction between all the stiffening elements, depend on the following parameters (see Table 4), which are considered in the DOE.

**Table 4:** Input parameters for the triangular cell optimization.

	Minimum	Initial	Maximum
Cantilever span L	150	150	150
Depth H [m]	0.2	0.6	0.8
Thickness $e_c$ [m]	0.020	0.025	0.035
Web Thickness $e_w$ [m]	0.020	0.025	0.035

The most relevant parameter is the web thickness, since the maximum load and the width of the launching support were established before. Fig. 10 shows the response surfaces of the main output parameters, web deflection (Fig. 10a) and web stress (Fig. 10b) depending on the height of the triangular cell and the thickness of the web.

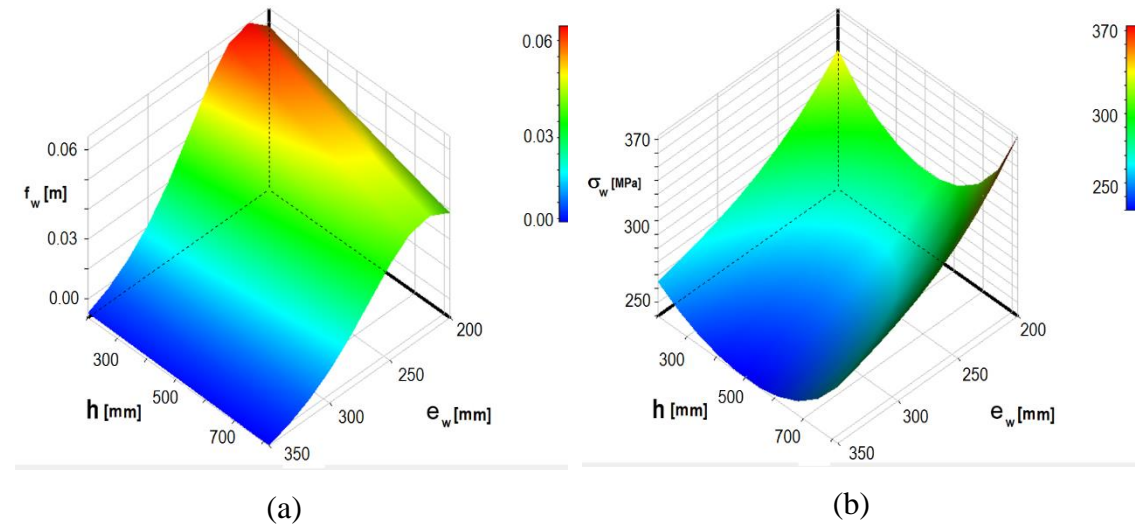


**Fig. 10.** Maximum displacement (a) and maximum stress (b) in the web vs web thickness and cell height.

A symmetric design of the triangular cell is adopted because the thickness of each plate (inside and outside) is not important enough and possible errors in the assembly of the steel structure are avoided. The results obtained, which comply with both conditions - web deflection and von Mises stress - are summarized in Table 5:

**Table 5:** Output results for the triangular cell optimization.

	Web thickness $e_w$	Cell thickness $e_c$	Cell height h
[m]	0.030	0.025	0,5

*3.2.4. Final Design, longitudinal stiffener position and depth of the stiffeners results*

A lot of references can be found in literature that try to define the best position of the longitudinal stiffener with respect to the bottom of a beam made of steel. Some boundary

conditions and loads are also extensively tested. Hence, this study takes the value of 30% web depth as the first step to carry out the DOE. In this case, the location of the longitudinal stiffener is the most important parameter from the web deflection point of view. Once the location is defined, the next most important parameter is the stiffener inertia. Table 6 and Fig. 11 shows the input parameters used for the stiffener optimization:

**Table 6:** Input parameters for the stiffener combination optimization.

	Minimal	Initial	Maximal
Cantilever span	150	150	150
Triangular cell depth $h$ [m]	0.5	0.5	0.5
Triangular cell thickness $e_c$ [m]	0.025	0.025	0.025
Web Thickness $e_w$ [m]	0.030	0.030	0.030
Long. stiffener height from bottom $h_{ls}$ [m]	2.5	2.7	3
Longitudinal stiffener depth $d_{ls}$ [m]	0.100	0.200	0.250
Vertical stiffener depth $d_{vs}$ [m]	0.100	0.200	0.300

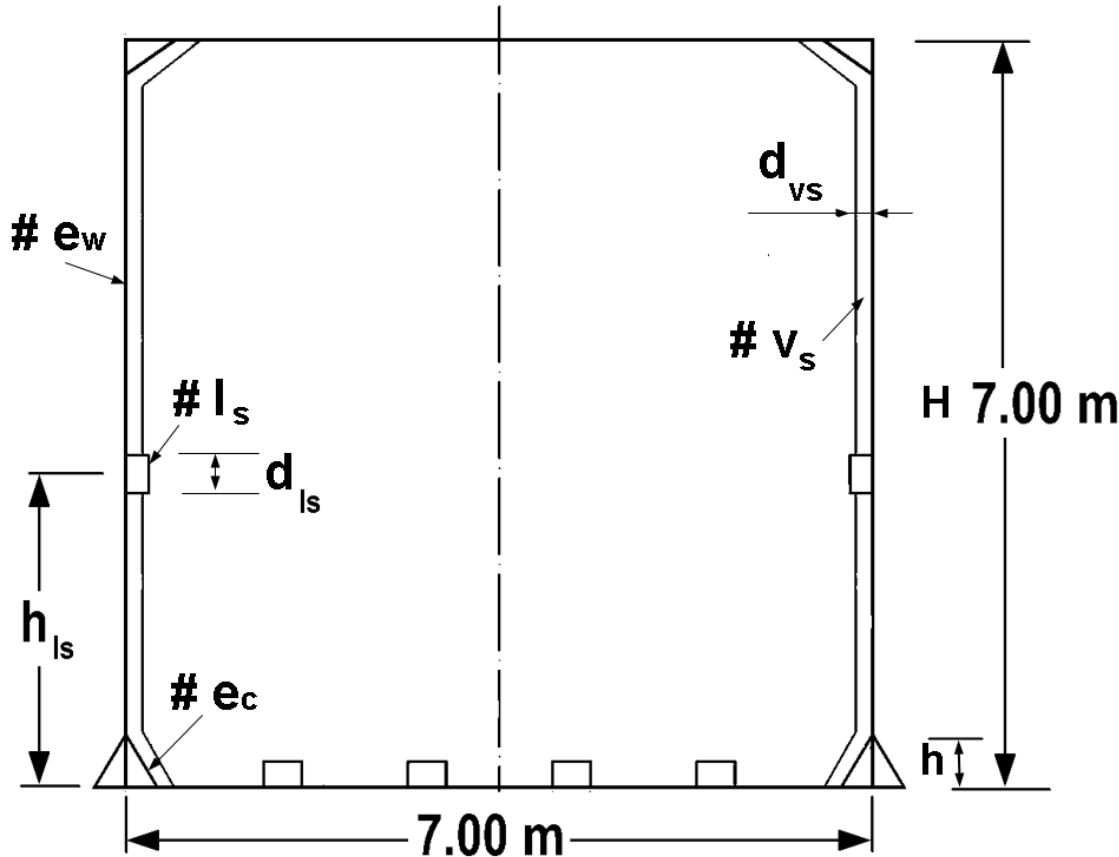


**Fig. 11.** Input parameters used for the stiffener optimization.

The maximum von Mises stress in the web remains virtually constant. The depth of both longitudinal and vertical stiffeners only control the stress in the elements themselves. As was seen in the previous analysis the stresses are always less than the elastic yield stress of steel. The fact that the whole design is being carried out with the objective of making the stresses lower than 60% of the yield stress of S-355 steel grade must be highlighted. Fig. 12 shows the sensitivity analysis results from the DOE, in which the relative influence of each input parameter on the outputs are shown:

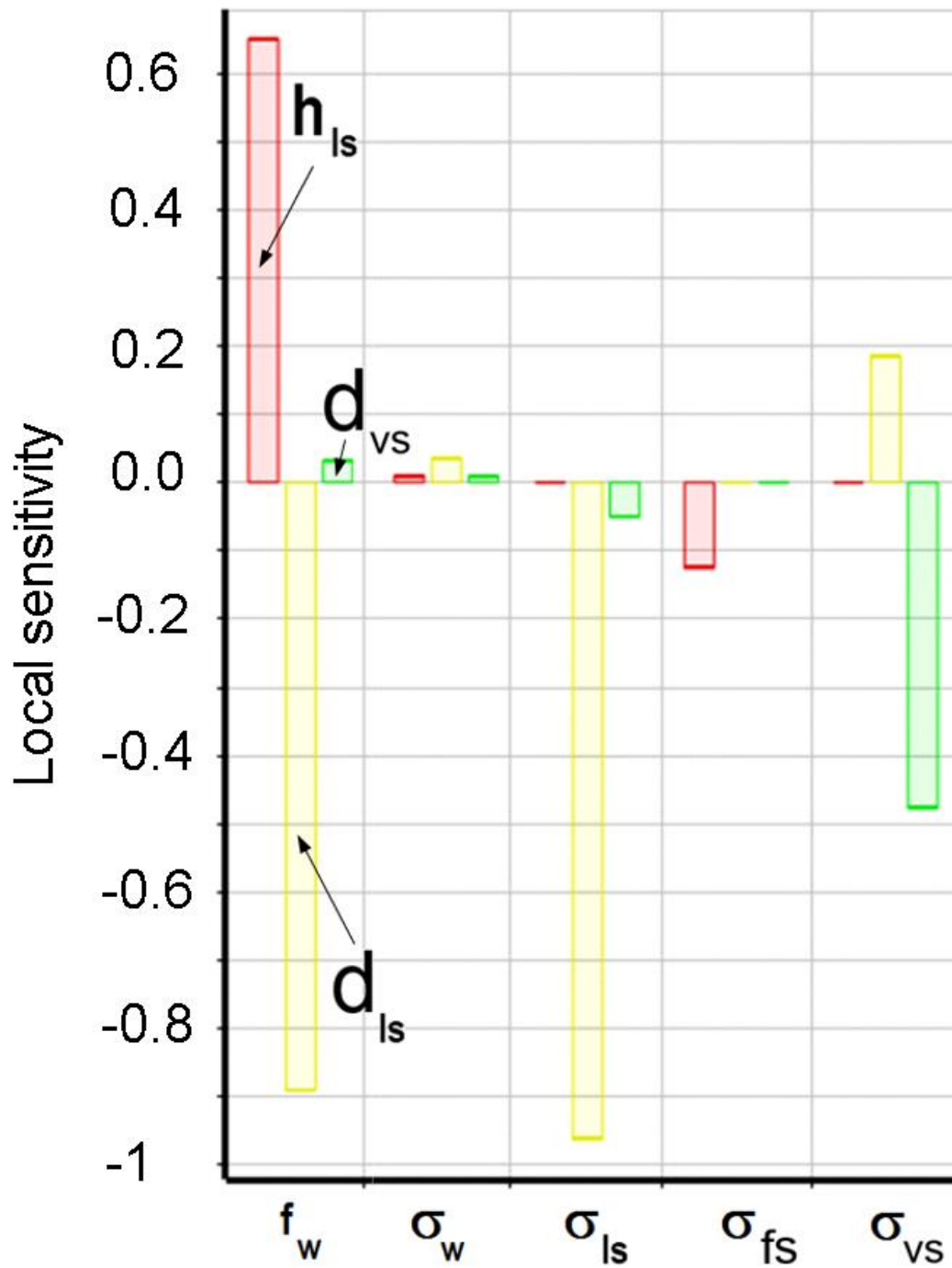


**Fig. 12.** Sensitivity analysis, showing the optimization of the longitudinal stiffness.

Fig. 13 contains the response surfaces of the output parameters, web deflection and stress on both longitudinal and vertical stiffeners:

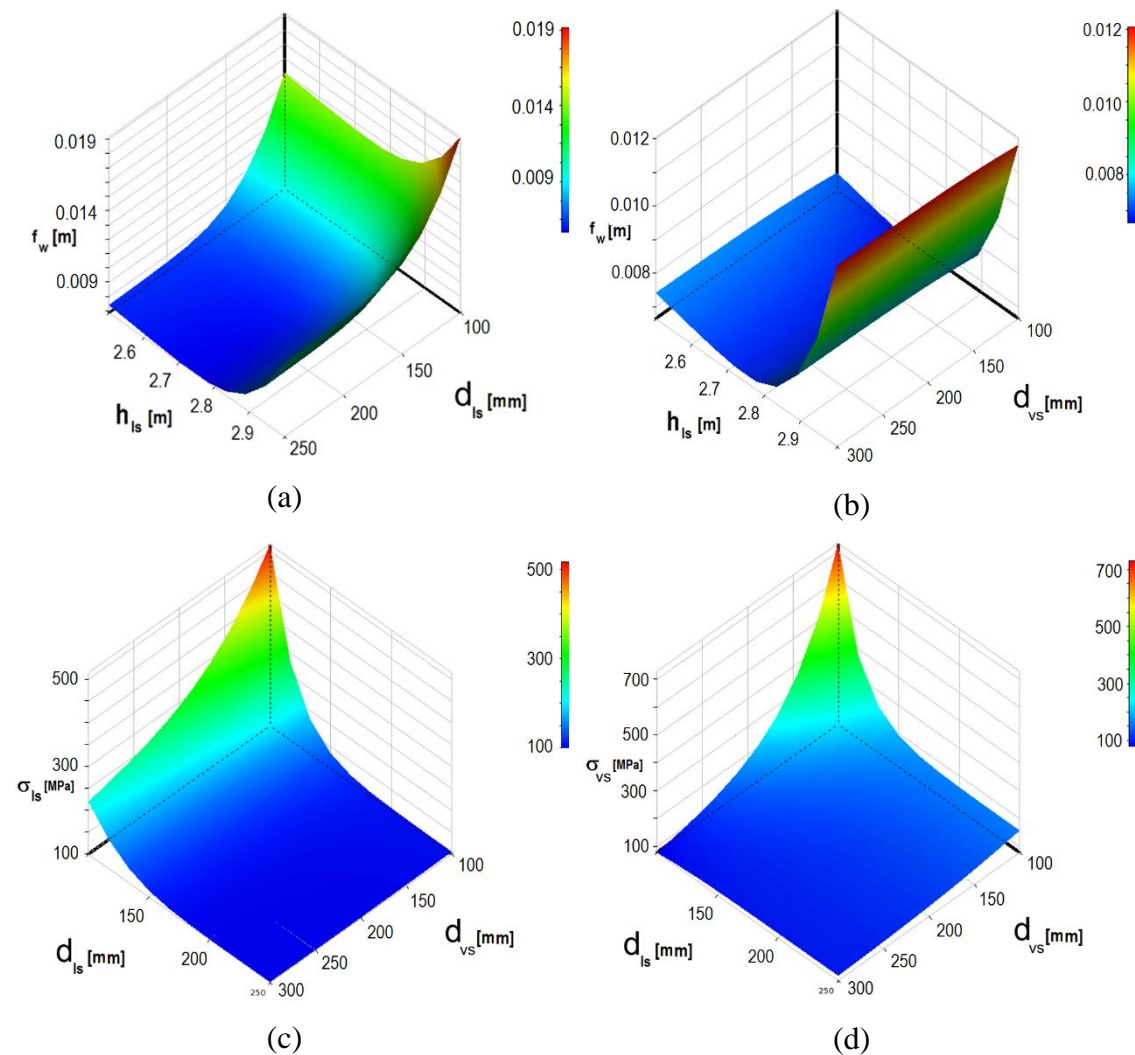


**Fig. 13.** Response surface results: (upper) web deflection vs. longitudinal stiffener location: (a) longitudinal stiffener height and (b) vertical stiffener height; (lower) (c) longitudinal and (d) vertical stiffener von Mises stress vs. longitudinal and vertical stiffener height.

The results obtained in the final bridge design are as follows (see Table 7):

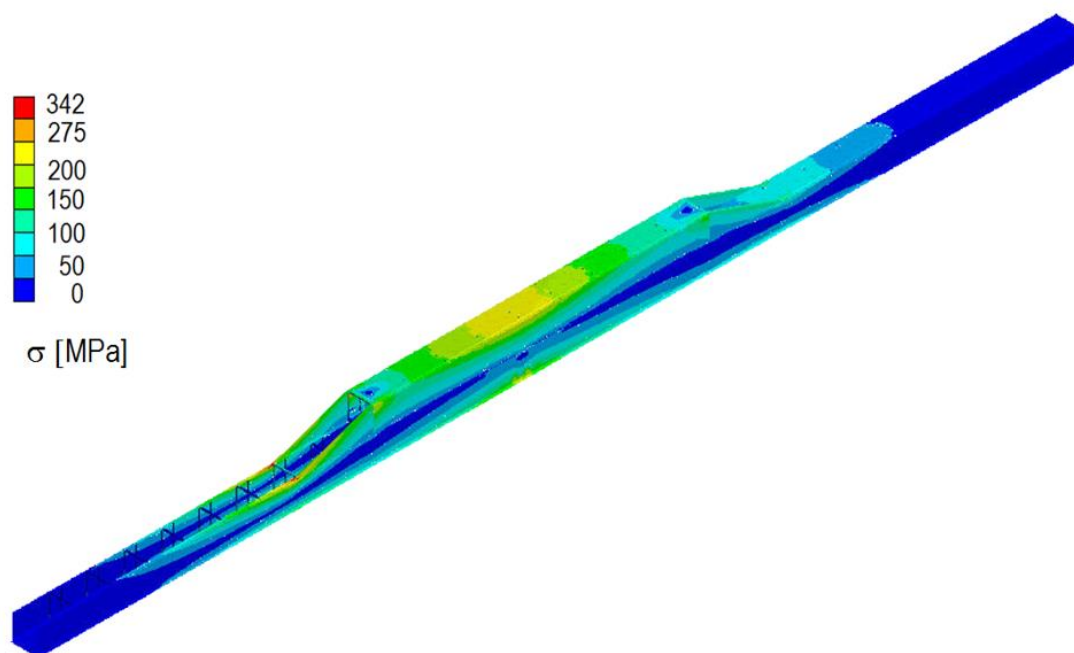
**Table 7:** Results for the stiffener combination optimization.

Maximum web thickness, $e_w$	30 mm
Maximum web thickness in the upper box (double-deck), $e_{wu}$	20 mm
Depth of the complete triangular cell, $h$	500 mm
Maximum thickness of the triangular cell, $e_c$	25 mm

Height of the longitudinal stiffener (from the bottom plate), $h_{ls}$	2.75 m
Dimensions of the longitudinal stiffener	320 x 200 x 8 mm
Dimensions of the vertical stiffeners (placed each 3.33 m)	7000 x 150 x 12 mm
Maximum web deflection $f_w$ (+)	0.00614 m
Maximum web deflection $f_w$ (-)	-0.00392 m
Maximum von Mises stress $\sigma$	342.8525 MPa
Total deflection at the launching nose $f$	2.39 m
Limit deflection/span $\frac{f}{2L}$	1/125
Maximum von Mises stress in the web $\sigma_w$	292.2148 MPa
Maximum von Mises stress in the outer triangular cell $\sigma_{co}$	276.2650 MPa
Maximum von Mises stress in the inner triangular cell $\sigma_{ci}$	258.1481 MPa
Maximum von Mises stress in the longitudinal stiffener $\sigma_{ls}$	102.2397 MPa
Maximum von Mises stress in transversal frames $\sigma_f$	281.1212 MPa
Maximum von Mises stress in vertical stiffeners $\sigma_{vs}$	79.2608 MPa
Eccentricity coefficient $\partial$	1.5
Maximum vertical reaction on support R1	14000 kN (1391.11Mp)
<b>Maximum vertical reaction on support R2</b>	<b>14000 kN (1388.5 Mp)</b>

As a result of these calculations, in order to optimize the double deck method, one longitudinal stiffener and two vertical stiffeners between two consecutive transversal frames were configured. Table 7 shows the values of all the parameters involved during the launching stage corresponding to the maximum cantilever position. Fig. 14 to 16 show the numerical results of the von Mises stress, the deflection of the structure and the detailed graph of the segment positioned directly over the pier during the critical launching phase.





526  
527

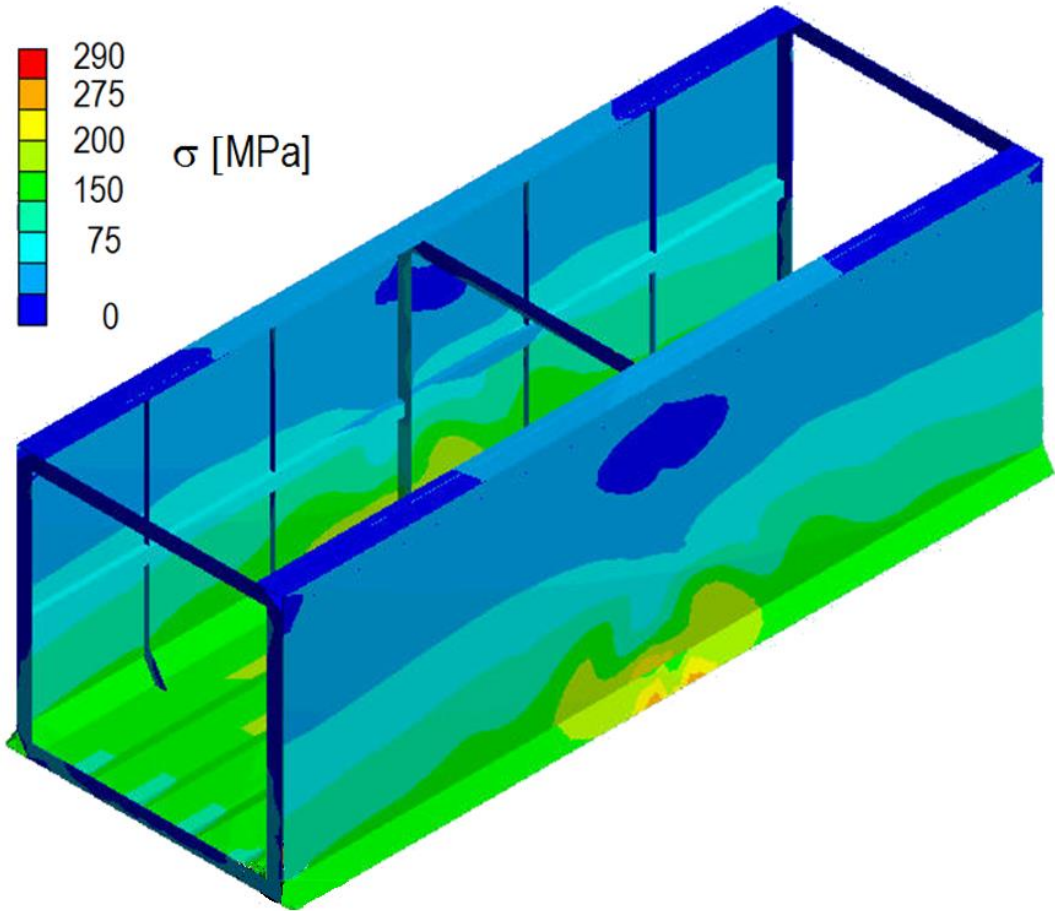


**Fig. 14.** Optimized von Mises stress, during the critical launching phase: overall view (upper) and segment directly over the pier (lower).

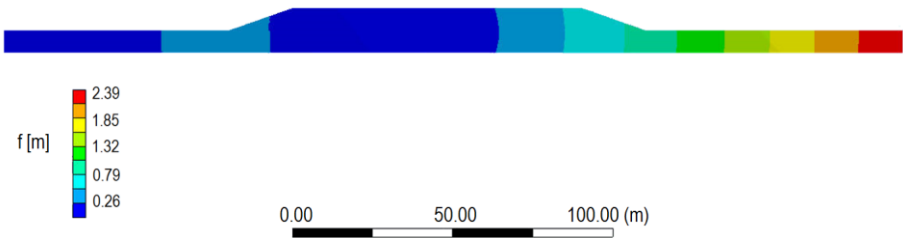


**Fig. 15.** Deflection, during the critical launching phase, 150 m cantilever span.

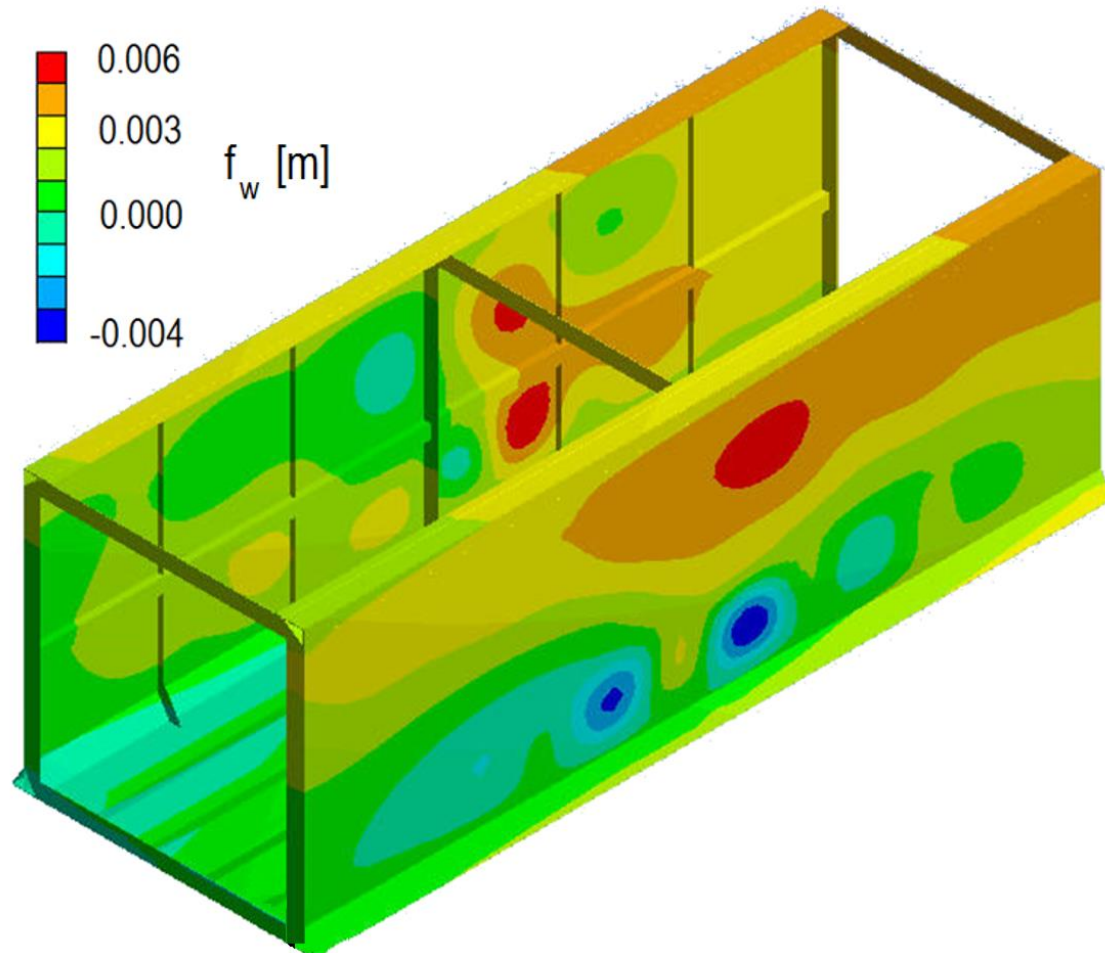


**Fig. 16.** Web deflection  $f_w$ , during the critical launching phase, segment directly over the pier.

#### 4. Conclusions

The aim of this paper is to present a study of the best way to stiffen a high depth bridge steel deck, and to apply it in a new launching method for steel bridges. The construction process must not be restrictive in the structural bridge design. Otherwise, material would be used in a non-efficient and non-sustainable way.

Taking into account the results of this paper, it has been found that a 150 m long span bridge can be launched by the double-deck procedure, without any auxiliary or non-reusable means.

Moreover, it has also been shown how the use of advanced simulation methods (combining the FEM and DOE techniques) provides the adequate structural response of a complex structure. The main parameters have been identified and a nonlinear numerical simulation by FEM has been carried out, making several numerical models and studying

them within a wide range of cases. The most important variables were then optimized by means of sensitivity analysis and design of experiments (DOE).

The principal conclusions are the following:

- The triangular cell along the down flange (both inside and outside the web) is a very important stiffener that contributes to patch loading resistance. Web stress is decreased by about 30% when  $20 \cdot 10^{-3}$  m thick plates are used.
- Many authors have proposed a maximum web height of 4 m to use the transversal stiffeners instead of longitudinal stiffeners. Nevertheless the optimum stiffener distribution consists of a combination of both longitudinal and transversal, called CASE-VI. There are two longitudinal stiffeners, one of them is the triangular cell and the other is located approximately at  $\frac{h}{3}$  from the deck bottom. The transversal stiffeners are vertical profiles, located between the transversal frames of the deck.
- Web deflection, one of the most important design parameters, mostly depends on the web thickness and the location of the second longitudinal stiffener.
- Web tensional states are controlled by the triangular cell along the down plate of the deck. Patch loading resistance is defined by this strong longitudinal stiffener which allows optimization of the web thickness along the whole deck.

The results then lead us to future investigations in many fields. After the analysis of a new launching method in this paper, the objective will be to analyze the effect of the real deflection of the steel beam in the reaction forces on both the piers and the pushing mechanism.

The authors suggest a future research line about the development of testing on prototype models of the bridge launched (e.g. scale 1:15) in order to calibrate more accurately the numerical simulations.

A high level of development along these research lines is current expected in order to regulate and integrate the different international codes regarding buckling formulation and bridge construction systems.

## 5. Acknowledgements

The authors of this paper greatly appreciate the collaboration of the GICONSIM Research Group at the University of Oviedo, the GITECO Research Group at the University of Cantabria, The Polytechnic University of Madrid, COPROSA Ltd, ULMA Ltd. and Torroja Ltd. and, specifically, to Víctor Orodea López, Javier Merino Rasines, Benjamín Navamuel García; José Simón Talero and Maximino Menéndez Cabo. Furthermore, the authors wish to acknowledge the financial support provided by the Spanish Ministry of Science and Innovation with funds from ALCANZA Research Project number IPT-380000-2010-12 and BIA-2012-31609. These projects have been co-

financed with FEDER funds, "A Way of Making Europe". Besides, we also thank Swanson Analysis Inc. for the use of the ANSYS University Research program and Workbench simulation environment. Finally, the authors wish to acknowledge the English editing work made by Andrew McCammond.

## 6. References

- [1]. Bernabeu Larena J. Typology and Aesthetic Evolution of the European Composite Bridges. Doctoral Thesis. Madrid UPM Department of Structural Engineering; Spain. 2004.
- [2]. German Patent DE1237603 (B). Verfahren zum herstellen von langen bauwerken, insbesondere bruecken, aus stahl-oder spannbeton. 1967.
- [3]. Rosignoli M. Bridge launching. London. Thomas Telford. 2002.
- [4]. Navarro-Manso A. A new steel bridge launching system based on self-supporting double deck: structural numerical simulation and wind tunnel tests. Doctoral Thesis. University of Cantabria; Spain 2013.
- [5]. Bouchon E. et al. Guide des ponts poussés. Presses de l'école nationale des ponts et chaussees. Paris. 1999.
- [6]. Petetin S. et al. Bulletin 23 Ponts Metalliques 2004. OUTA. Paris. 2004.
- [7]. La Violette M. et al. Bridge construction practices using incremental launching. AASHTO. Washington. D. C. 2007.
- [8]. Alonso-Martínez M. New device for continuous launching of bridge structures: design and analysis using numerical simulation. Doctoral Thesis. University of Oviedo. Spain. 2013.
- [9]. De Matteis D. et al. Steel-Concrete Composite Bridges, Sustainable Design Guide. SETRA Ministere de l'Ecologie, de l'Energie, du Developpement durable et de la Mer. France. 2010.
- [10]. Kuhlmann U. et al. COMBRI Design Manual. Part II: State-of-the-Art and Conceptual Design of Steel and Composite Bridges. Research Fund for Coal and Steel and University of Stuttgart. Institute of Structural Design. European Commission. 2008.
- [11]. International Patent WO 2013/001115 A1. System and method for launching structures. 2012.
- [12]. International Patent WO 2013/001114 A1. Device to continuous displacement of structures. 2012.
- [13]. Lagerqvist O. Patch loading: resistance of steel girders subjected to concentrated forces. Doctoral thesis. Lulea University. Sweden. 1994.
- [14]. Granath P. Serviceability limit state of I-shaped steel girders subjected to patch loading. *J Const Steel Res* 2000; 54(3): 387-408.
- [15]. Graciano C, Edlund B. Failure mechanism of slender girder webs with a longitudinal stiffener under patch loading. *J Const Steel Res* 2003;59(1):27–45.
- [16]. Hajdin N, Markovic N. Failure mechanism for longitudinally stiffened I girders subjected to patch loading. *Archive of Applied Mechanics* 2012;82:1377–91.
- [17]. Marchetti M.E. Specific design problems related to bridges built using the incremental launching method. *Eng Struct* 1984; 6: 185-210.

- [18]. Graciano C. Patch loading: Resistance of longitudinally stiffened steel girder webs. Doctoral thesis. Lulea University of Technology. Sweeden. 2001.
- [19]. Navarro-Manso A., Del Coz Diaz J.J., Alonso Martinez M., Castro-Fresno D., Blanco-Fernández E. New launching method for steel bridges based on a self-supporting deck system: FEM and DOE analysis. *Autom Constr* 2014; 44: 183-196.
- [20]. Alonso-Martínez M., del Coz Díaz J.J., Navarro-Manso A., Castro-Fresno D. Bridge-structure interaction analysis of a new bidirectional and continuous launching bridge mechanism. *Eng Struct* 2014; 59: 298-307.
- [21]. Alonso-Martínez M., del Coz Díaz J.J., Castro-Fresno D., Navarro-Manso A. New mechanism for continuous and bidirectional displacement of heavy structures: Design and analysis. *Autom Constr* 2014; 44: 47-55.
- [22]. ANSYS, Inc, ANSYS Release 12.0 Elements Reference, USA; 2009.
- [23]. Graciano C, Edlund B. Nonlinear FE analysis of longitudinally stiffened girder webs under patch loading. *J Const Steel Res* 2002;8:1231–1245.
- [24]. Millanes Mato F., Pascual Santos J., Ortega Cornejo M. Arroyo las Piedras viaduct: The first Composite Steel-Concrete High Speed Railway Bridge in Spain. *Hormigón y Acero* 2007; 243: 5-38.
- [25]. ASME BPVC-Rules for Construction of Pressure Vessels Division 2-Alternative Rules. ASME. USA. 2013.
- [26]. UNE - EN 1993-1-5. Design of steel structures. Part 1-5: Plated structural elements. AENOR. Madrid. 2008.
- [27]. Gozzi J. Patch loading: Resistance of plated girders. Ultimate and serviceability limit state. Doctoral thesis. Lulea University of Technology Sweeden. 2007.
- [28]. Chacon R., Mirambell E., Real E. Influence of designer-assumed initial conditions on the numerical modelling of steel plate girders subjected to patch loading. *Thin-Walled Struct* 2009; 47(4): 391-402.
- [29]. del Coz Díaz J.J., Álvarez Rabanal F.P., García Nieto P.J., Rocas-García J., Alonso-Estébanez A. Nonlinear buckling and failure analysis of a self-weighted metallic roof with and without skylights by FEM. *Eng Fail Anal* 2012; 26: 65-80.
- [30]. del Coz Díaz J.J., Serrano López M.A., López-Colina Pérez C., Álvarez Rabanal F.P. Effect of the vent hole geometry and welding on the static strength of galvanized RHS K-joints by FEM and DOE. *Eng Struct* 2012; 41: 218-233.
- [31]. Box G, Hunter W, Hunter J. Statistics for experimenters. Second Ed. Wiley, 2005.
- [32]. D.C. Montgomery, Design and Analysis of Engineering Experiments, 5th ed., John Wiley & Sons, New York, 2001.
- [33]. R.H. Myers, D.C. Montgomery, Response Surface Methodology: Process and Product Optimization Using Designed Experiments, 2nd ed., John Wiley & Sons, New York, 2002.